INFRARED VARIABILITY OF SS 433

KEIICHI KODAIRA
Tokyo Astronomical Observatory, University of Tokyo

Y. NAKADA
Department of Astronomy, Faculty of Science, University of Tokyo

AND

D. E. BACKMAN
Institute for Astronomy, University of Hawaii
Received 1984 December 6; accepted 1985 March 8

ABSTRACT

New *JHKLM* photometry of SS 433 showing short time scale variabilities is reported for the period of 1983 July 16–22 UT. The entire body of infrared data included in this paper, Giles *et al.*, and Catchpole *et al.* is examined with reference to periods of 164 days and 13.08 days. Comparison of the infrared light curves with the optical light curves of Leibowitz *et al.* allows us to conclude, within the context of an accretion disk model, that the majority of the infrared flux in the SS 433 system comes from the disk, and that the hot spot responsible for the "hump" in the visual and infrared light curves has a color similar to the average of the disk. A two-dimensional Fourier analysis of the infrared data suggests that the brightness maximum occurs when, seen from the compact star, the noncompact companion passes through a fixed elongation relative to the disk line of nodes with the orbital plane, if the precession is prograde.
Subject headings: infrared: sources — stars: individual

I. INTRODUCTION

The extraordinary emission-line object SS 433 was found to be variable in the infrared region on a time scale of days by Wynn-Williams and Becklin (1979) and by Milone and Clark (1979; Clark and Milone 1981). Later long-term infrared monitoring of this object by Giles *et al.* (1980) and by Catchpole *et al.* (1981) indicated variabilities with periods of 11.8 days and 165.5 days respectively. Kodaira and Lenzen (1983) found indications of infrared variability with a time scale of hours or less, which had been suspected by Clark and Milone (1981). The present paper reports the results of infrared monitoring of SS 433 in 1983 July undertaken to cover the phases of the long-term periods not yet observed, and also to confirm the short-term variabilities. The entire body of infrared data will be rediscussed in light of the recent analyses of photometric and spectroscopic observations in the optical region that revealed 164 day and 13.08 day periods (Leibowitz *et al.* 1984; Crampton and Hutchings 1981). A detailed study of empirical models of the SS 433 system based on the present photometry is under way and will be published separately.

II. OBSERVATION AND RESULTS

Near-infrared observations of SS 433 were carried out with the InSb photometer in the WMS-02 cryostat attached to the 2.2 m reflector of the University of Hawaii at Mauna Kea on 1983 July 16–22 UT. The photometry was done using a diaphragm of 5″ and with 10 Hz chopping between locations separated by 30″. The data were averaged over 5–30 sets of differences between pairs of successive 4 s integrations (with a 2 s dead-time interval) taken at beam-switching positions 30″ apart. The nearby photometric standard star BS 7429 ($J = 2.56$, $H = 2.01$, $K = 1.83$, $L = 1.70$, $M = 1.85$) served as the comparison object and was observed in alternation with SS 433, almost always at close intervals. The signal-to-noise ratios of the averaged integrated data were about 50(J), 50(H), 100(K), 20(L), and 5(M) for SS 433, and sufficiently high for the comparison star. The filters used were standard ones except for that of the L band, which in the WMS-02 cryostat is L' ($\lambda_0 = 3.8$ μm). The L magnitude of SS 433 was derived simply through the equation L(SS 433) = L'(BS 7429) + L(SS 433) − L'(BS 7429). The observational results are given in Table 1. The mean values of the internal random errors are about 0.01, 0.02, 0.01, 0.03, and 0.2 mag for the J, H, K, L, and M bands respectively. The correction for atmospheric extinction was performed by fitting a linear relation to the air mass using the standard star data. The standard deviations in these fits are given in Table 2 as a measure of the sky and instrumental stability.

III. LIGHT CURVES

The observation dates corresponded to phases $\Psi_{165.5} = 0.955$–0.992 for the IR ephemeris of Catchpole *et al.* (1981; $P = 165.5$ days and $T_0 = 2,443,718.9$ JD), and to phases $\Psi_{164} = 0.923$–0.961 and $\phi_{13} = -0.123$ to $+0.354$ for the ephemeris of Leibowitz *et al.* (1984; $P = 164$ days and 13.08 days and $T_0 = 2,444,068.5$ JD). In the following we adopt the latter ephemeris in order to compare the infrared observations with the *UBV* photometry summarized by Leibowitz *et al.* (1984). In this ephemeris the primary- and secondary-maximum separations of moving emission lines occur around $\Psi_{164} = 0.54$ and 0.04, respectively, and the crossover occurs around $\Psi_{164} = -0.12$ and 0.20 (cf. Margon 1982). The primary and secondary photometric minima in the optical region for phases $0.333 \leq \Psi_{164} \leq 0.666$ occur at $\phi_{13} = 0.23$ and 0.73 respectively (cf. Leibowitz *et al.* 1984).

The infrared light variations derived by combining the present data with the data given in Giles *et al.* (1980) and Catchpole *et al.* (1981) are shown in Figures 1–4 for the representative examples of the J and K bands. The smoothed mean variations are indicated by solid curves. The groupings

TABLE 1

JHKLM PHOTOMETRY OF SS 433

| N	UT (1983 July)	JD (2,445,500+)	Ψ_{164}	ϕ_{13}	J	H	K	L	M
1	16 0830	31.854	0.923	−0.123	...	...	8.02	7.00	6.58
2	0900	31.873	0.923	−0.121	9.37	8.78	8.00	6.99	6.38
3	0920	31.888	0.923	−0.120	9.39	8.85	8.03	6.97	6.14
4	0938	31.900	0.923	−0.119	9.44	8.81	...	...	...
5	1011	31.923	0.923	−0.118	9.45	8.89	8.05	7.06	6.59
6	1029	31.935	0.923	−0.117	9.43	8.91	8.06	7.00	6.55
7	1045	31.946	0.923	−0.116	9.50	8.89	8.05	7.05	6.51
8	17 1020	32.929	0.929	−0.041	9.44	8.86	8.05	6.96	6.58
9	1044	32.946	0.930	−0.039	9.54	8.87	8.08	6.96	6.81
10	1121	32.971	0.930	−0.037	9.52	8.86	8.06	6.90	6.50
11	1153	32.995	0.930	−0.036	9.57	...	...	...	...
12	1208	33.004	0.930	−0.035	9.66	8.96	8.18	7.11	6.84
13	1232	33.021	0.930	−0.034	9.62	8.86	8.14	7.03	6.51
14	1245	33.029	0.930	−0.033	9.70	9.05	8.38	7.13	6.70
15	1308	33.046	0.930	−0.032	9.60	8.95	8.15	7.23	6.53
16	1321	33.056	0.930	−0.031	...	...	8.22	7.03	6.37
17	1402	33.084	0.930	−0.029	9.63	9.18	...	...	6.81
18	1416	33.093	0.930	−0.028	9.59	9.03	8.28	7.19	...
19	18 1349	34.075	0.936	+0.047	9.44	8.60	8.10	7.03	7.16
20	1412	34.091	0.937	+0.048	9.46	8.61	...	7.09	6.58
21	19 0637	34.774	0.941	+0.100	9.40	8.81	8.08	7.03	...
22	0910	34.887	0.941	+0.109	9.43	8.79	8.05	7.06	6.67
23	0940	34.908	0.941	+0.110	...	...	...	7.04	...
24	1111	34.965	0.942	+0.115	9.35	8.76	7.98	6.92	6.83
25	1131	34.978	0.942	+0.116	9.38	8.79	8.01	6.93	6.65
26	1200	34.999	0.942	+0.118	9.43	8.74	7.99	7.00	...
27	1231	35.021	0.942	+0.119	9.45	8.79	8.08	6.97	6.37
28	1306	35.046	0.942	+0.121	9.44	8.81	8.05	6.93	...
29	1309	35.048	0.942	+0.121	...	...	8.09	...	...
30	1335	35.065	0.942	+0.123	9.39	8.78	8.05	6.92	6.44
31	1356	35.079	0.943	+0.124	9.34	8.74	7.99	6.97	...
32	1419	35.096	0.943	+0.125	9.40	8.80	8.00	6.98	6.73
33	20 0622	35.760	0.947	+0.176	9.50	8.97	8.43	7.31	...
34	0636	35.774	0.947	+0.177	9.48	8.92	8.19	7.16	7.42
35	0711	35.798	0.947	+0.178	9.49	8.96	8.25	7.11	6.94
36	0731	35.812	0.947	+0.180	9.44	8.88	8.15	7.11	6.96
37	0752	35.827	0.947	+0.181	9.42	8.87	8.15	7.08	7.04
38	0813	35.841	0.947	+0.182	9.59	8.91	8.24	7.23	7.32
39	0834	35.855	0.947	+0.183	9.62	9.03	8.22	7.23	6.99
40	0852	35.868	0.947	+0.184	9.62	9.01	8.30	7.25	6.98
41	0853	35.869	0.947	+0.184	...	...	8.26	...	...
42	0854	35.870	0.947	+0.184	...	...	...	7.35	...
43	0856	35.872	0.947	+0.184	...	...	...	7.29	...
44	0915	35.884	0.947	+0.185	9.52	8.96	8.24	7.19	6.95
45	0933	35.897	0.948	+0.186	9.57	9.05	8.23	7.25	7.05
46	0954	35.911	0.948	+0.187	9.52	8.99	8.23	7.34	6.83
47	1023	35.931	0.948	+0.189	9.53	8.98	8.23	7.14	6.68
48	1052	35.946	0.948	+0.190	9.46	8.89	8.15	7.06	6.67
49	1117	35.969	0.948	+0.192	9.48	8.95	8.19	7.10	6.57
50	1153	35.994	0.948	+0.194	9.48	8.89	8.19	7.13	...
51	1218	36.011	0.948	+0.195	9.51	8.91	8.17	7.12	6.90
52	1238	36.025	0.948	+0.196	9.42	8.87	8.16	7.13	6.68
53	1301	36.041	0.948	+0.197	9.48	8.89	8.15	7.08	7.23
54	1319	36.054	0.948	+0.198	9.44	8.85	8.13	7.02	6.93
55	1339	36.068	0.949	+0.199	9.53	8.89	8.17	7.15	6.71
56	1400	36.082	0.949	+0.200	9.47	8.88	8.14	7.09	6.42
57	21 0829	36.852	0.953	+0.259	9.47	8.92	8.12	7.04	7.68
58	0854	36.869	0.953	+0.261	9.52	8.95	8.16	7.15	6.76
59	0916	36.885	0.954	+0.262	9.50	8.97	8.16	7.17	...
60	1322	37.051	0.955	+0.275	9.43	8.87	8.09	7.00	...
61	1344	37.071	0.955	+0.276	9.44	8.89	8.10	6.90	...
62	1403	37.084	0.955	+0.277	9.46	8.91	8.12	7.06	...
63	22 0619	37.761	0.959	+0.329	9.54	8.89	8.15	7.11	6.30
64	0648	37.781	0.959	+0.330	9.52	8.91	8.14	7.06	6.75
65	0711	37.798	0.959	+0.332	9.57	8.99	8.23	7.12	7.06
66	0730	37.811	0.959	+0.333	9.54	9.00	8.24	7.12	...
67	0754	37.828	0.959	...	...	9.05	8.25	7.07	6.64
68	0817	37.844	0.959	+0.335	9.61	9.02	8.27	7.23	6.48
69	1308	38.056	0.961	+0.351	9.68	9.03	8.13	7.15	6.36
70	1327	38.072	0.961	+0.353	9.68	9.05	8.10	7.10	6.27
71	1345	38.088	0.961	+0.354	9.47	9.00	8.06	7.22	6.16
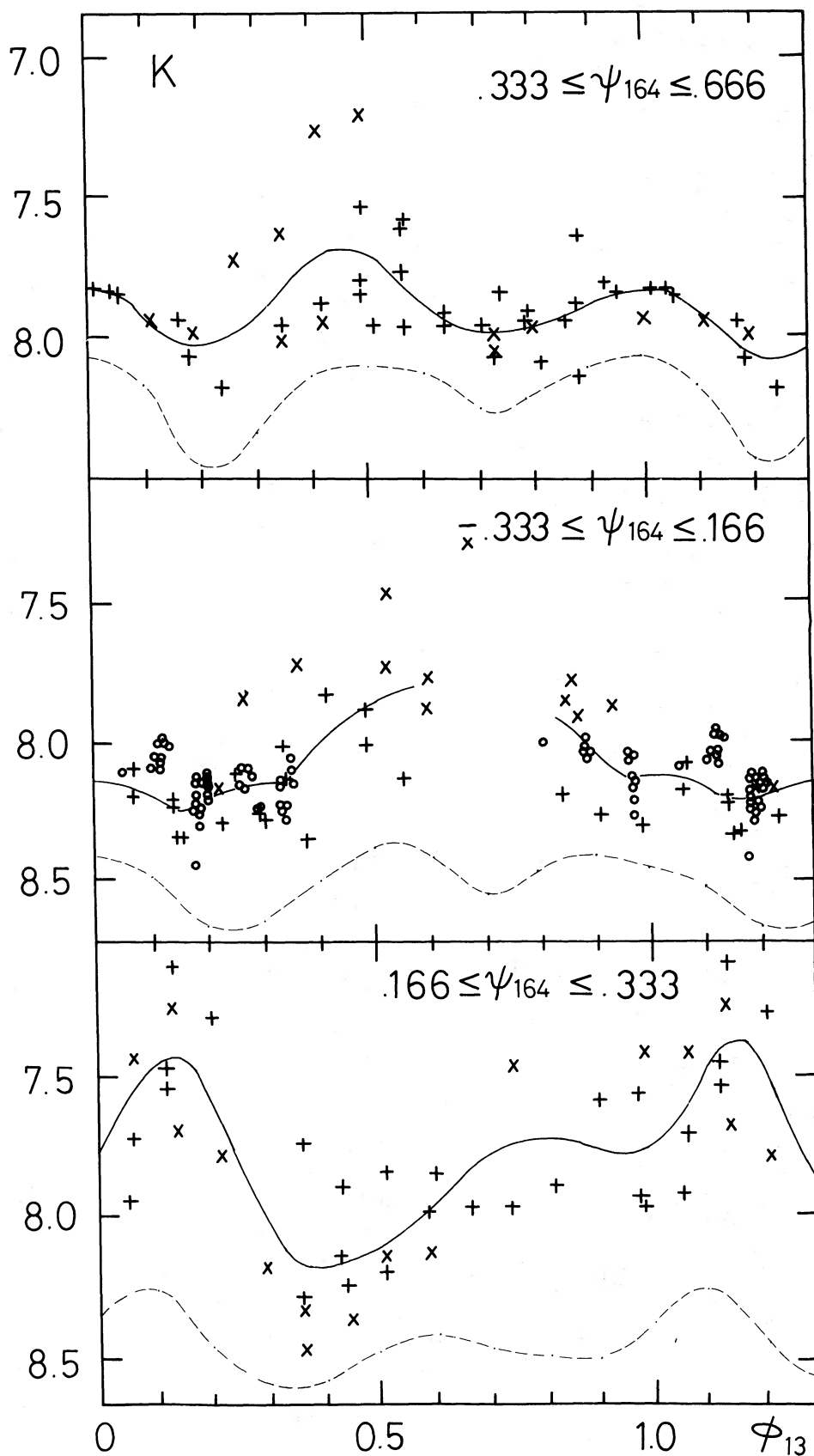
FIG. 1.—The 13.08 day light curve of SS 433 in the K band, in three phase intervals of the 164 day cycle. Symbols are × for Giles *et al.* (1980), + for Catchpole *et al.* (1981), and ○ for the present paper. The solid curves represent the mean variation and the dashed curves indicate the mean variation in the V band of Leibowitz *et al.* (1984), scaled by a factor of 0.6 with arbitrary zero points.
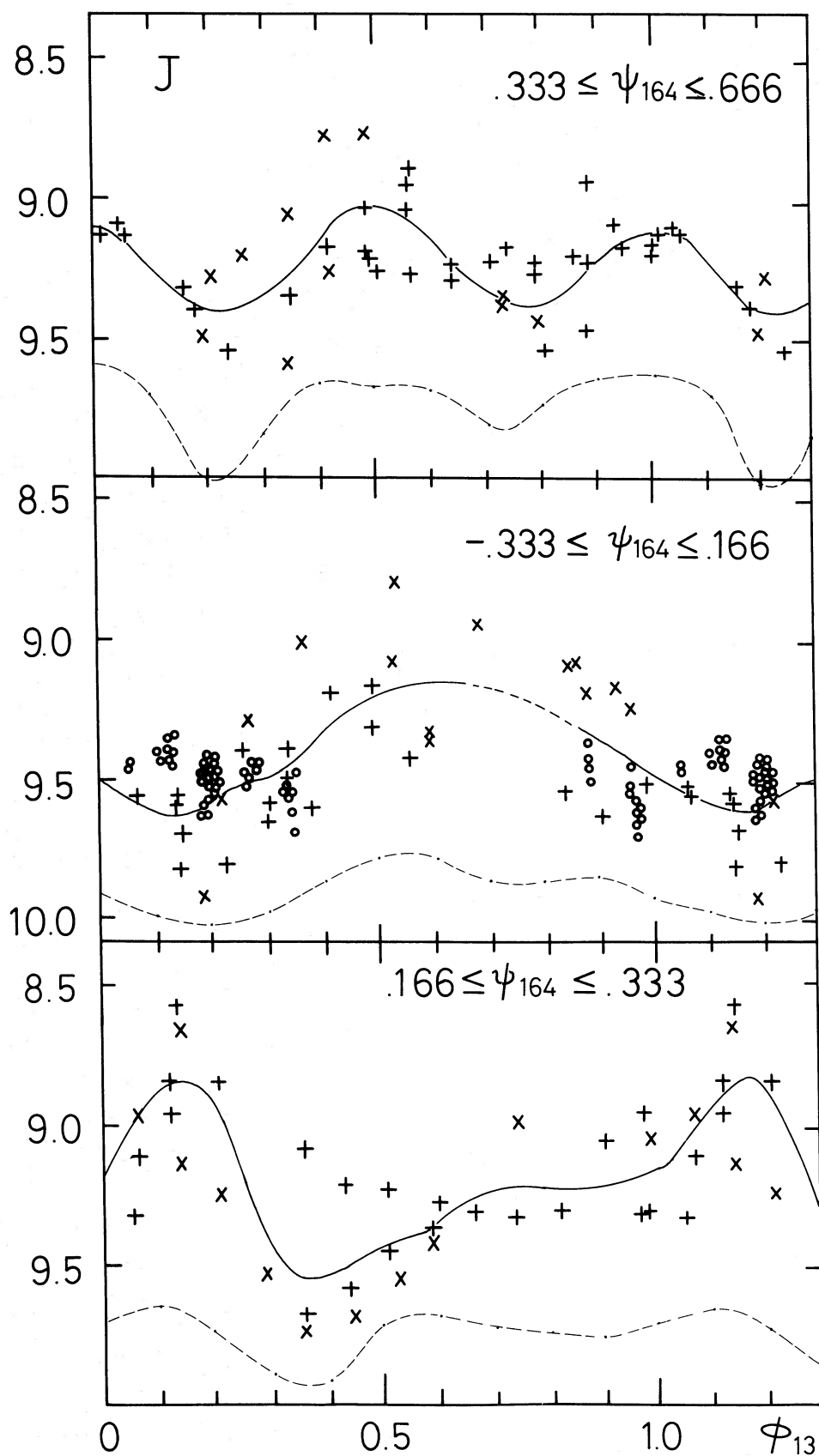
234

FIG. 2.—The 13.08 day light curve of SS 433 in the *J* band, in three phase intervals of the 164 day cycle. Symbols are the same as in Fig. 1. The dashed curves indicate the mean variation in the *B* band of Leibowitz *et al.* (1984), scaled by a factor of 0.6 with arbitrary zero points.

235

TABLE 2

STANDARD DEVIATIONS IN DETERMINATIONS OF THE ATMOSPHERIC
EXTINCTION COEFFICIENTS USING THE PHOTOMETRIC STANDARD
STAR BS (mag) 7429

	DATE (1983 July UT)						
BAND	16	17	18	19	20	21	22
J	0.03	0.02	0.04	0.02	0.03	0.01	0.02
H	0.04	0.04	0.02	0.05	0.02	0.01	0.04
K	0.03	0.04	0.04	0.03	0.03	0.01	0.02
L'	0.03	0.04	0.06	0.02	0.03	0.02	0.01
M	0.04	0.06	0.03	0.04	0.04	0.08	0.04

according to phase in these figures are the same as those in
Figures 5–8 of Leibowitz *et al.* (1984) for convenience of com-
parison; their light curves in V and B (scaled by a factor of 0.6)
are indicated by dashed curves in the lower parts of the figures.
The mean curves for the V and B bands are derived from the
raw data by a "cleaning" procedure (cf. Leibowitz *et al.* 1984),
while no "cleaning" is applied to the J or K data.

First of all, we notice for the 164 day period that (1) the light
curves are very similar at J and K, (2) the infrared and optical
patterns resemble each other, but (3) the infrared light curves
have about half the amplitude of the optical curves. One
obtains an impression that (4) the "hump" around $\Psi_{164} =$
0.2–0.3 is stronger in the infrared than in the optical region,
relative to the maximum around $\Psi_{164} = 0.5$. As for the light
curves over the 13.08 day period, (5) the minima around $\phi_{13} =$
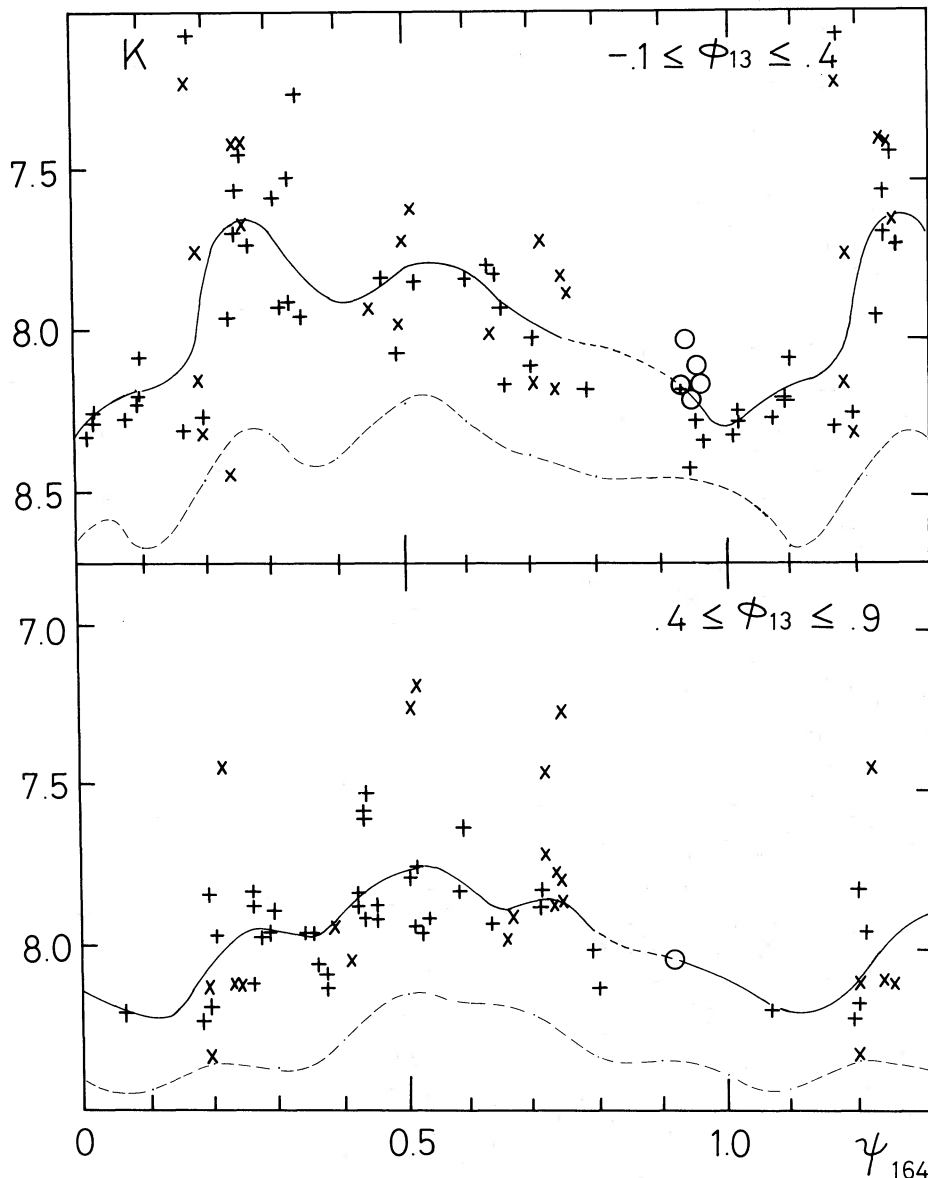
FIG. 3.—The 164 day light curve of SS 433 in the K band, in two halves of the 13.08 day cycle. Symbols are the same as in Fig. 1, except for the circles, which here
represent night means instead of individual values. The dashed curves indicate the mean variation in the V band of Leibowitz *et al.* (1984), scaled by a factor of 0.6
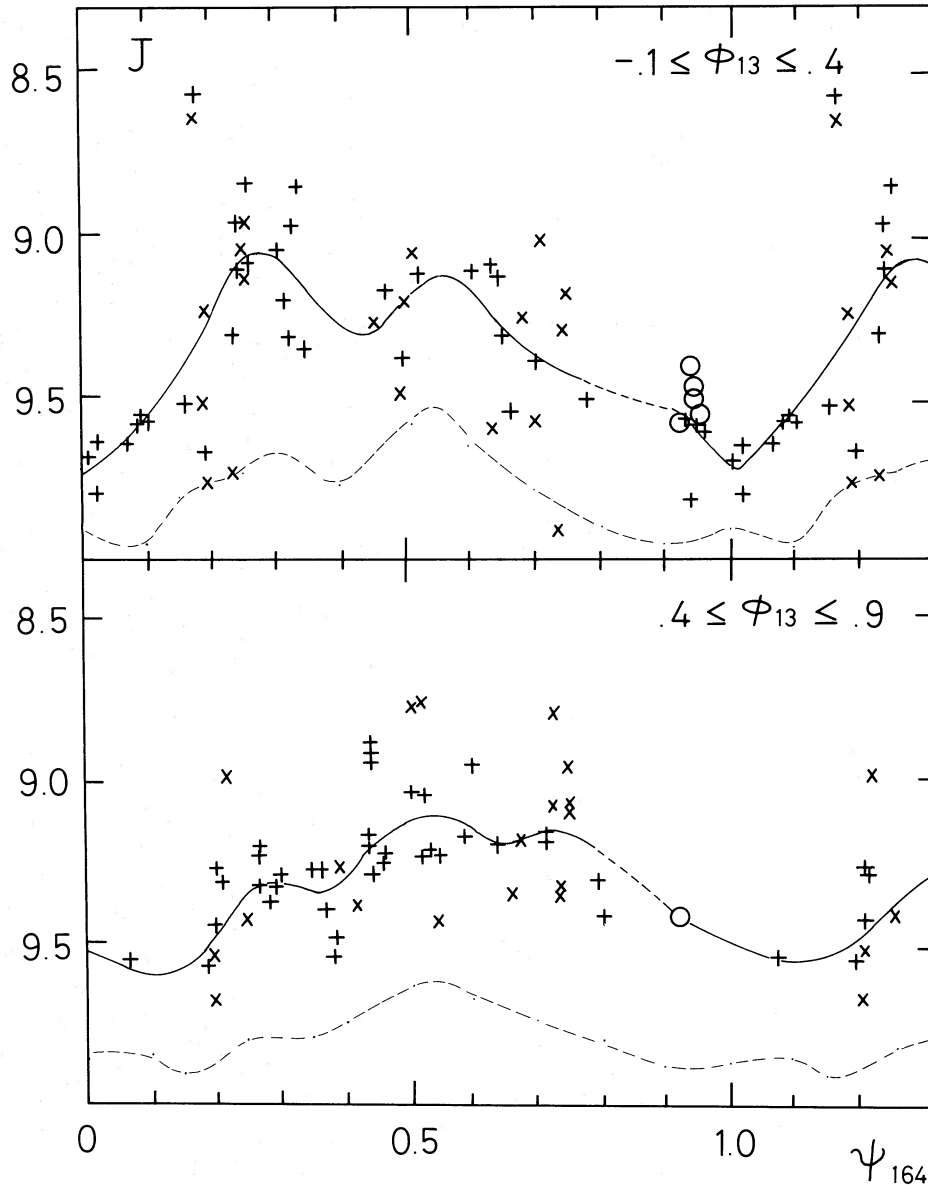with arbitrary zero points.

FIG. 4.—The 164 day light curve of SS 433 in the J band, in two halves of the 13.08 day cycle. Symbols are the same as in Fig. 3. The broken curves indicate the mean variation in the B band of Leibowitz *et al.* (1984), scaled by a factor of 0.6 with arbitrary zero points.

0.23 and 0.73 for $0.333 \leq \Psi_{164} \leq 0.666$ are shallow in the infrared, while (6) the anomalous modulations with peaks around $\phi_{13} \approx 0.5$ for $-0.333 \leq \Psi_{164} \leq 0.166$ and around $\phi_{13} \approx 0.1$ for $0.166 \leq \Psi_{164} \leq 0.333$ are nearly as strong at J and K as in the optical region, although the secondary peaks are not well recognizable. By achieving optimal overlapping of the J and K diagrams, we find that (7) the mean color index $J - K$ of light curves over the 13.08 day period is $+1.35 \pm 0.03$ $(0.333 < \Psi_{164} < 0.666)$, $+1.39 \pm 0.03$ $(-0.333 < \Psi_{164} < 0.166)$, and $+1.40 \pm 0.03$ $(0.666 < \Psi_{164} < 0.333)$; the mean infrared color is marginally bluer for phases $0.333 < \Psi_{164} < 0.666$.

IV. SHORT TIME SCALE VARIATION

The observations by Giles *et al.* (1980) and by Catchpole *et al.* (1981) revealed day-to-day fluctuations of infrared flux of a few tenths of a magnitude. The present data in the middle

panels of Figures 1 and 2 show the same kind of variations, and also substantial variations within single nights (July 17 and 20 UT). The flux distributions are plotted in Figure 5 using the calibration of Beckwith *et al.* (1976). The fluxes are averaged for each night (Fig. 5a) except for July 17 and 20 UT, for which "low" and "high" states are also shown separately (Fig. 5b). The "low" state has a time scale of 1 hr and shows little or no systematic color differences relative to the "high" state. These characteristics are similar to those reported by Kodaira and Lenzen (1983). The number of observations on July 18 was small and the flux curve for that night might be subject to large uncertainty. Nevertheless, the two data sets in Table 1 for July 18 coincide with each other very well and the excess in the H band may be significant. The infrared color was $J - K \approx 1.4$ on July 16 UT, became bluer ($J - K \approx 1.3$) on July 20 UT, and almost recovered to the initial state on July 22 UT. This color change was caused by the apparent excess in the J and H
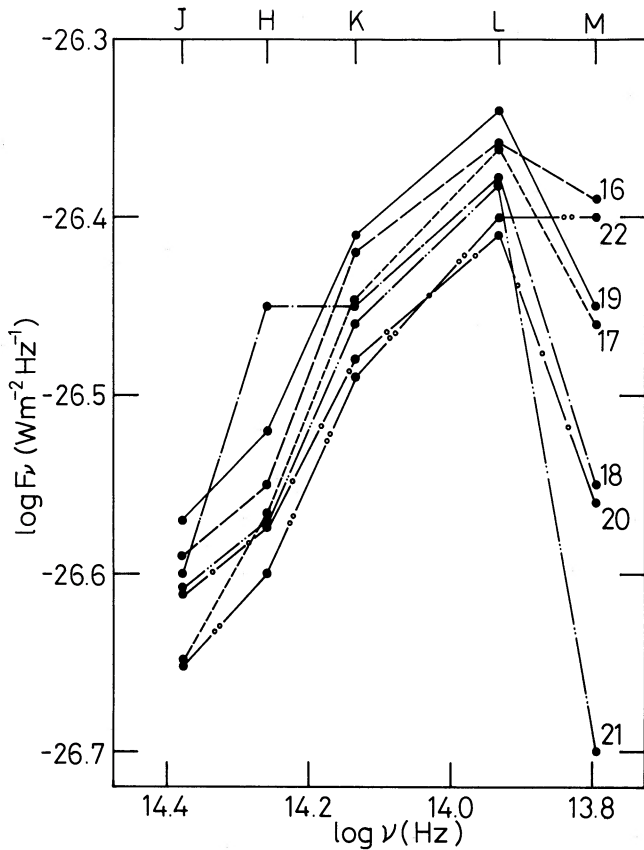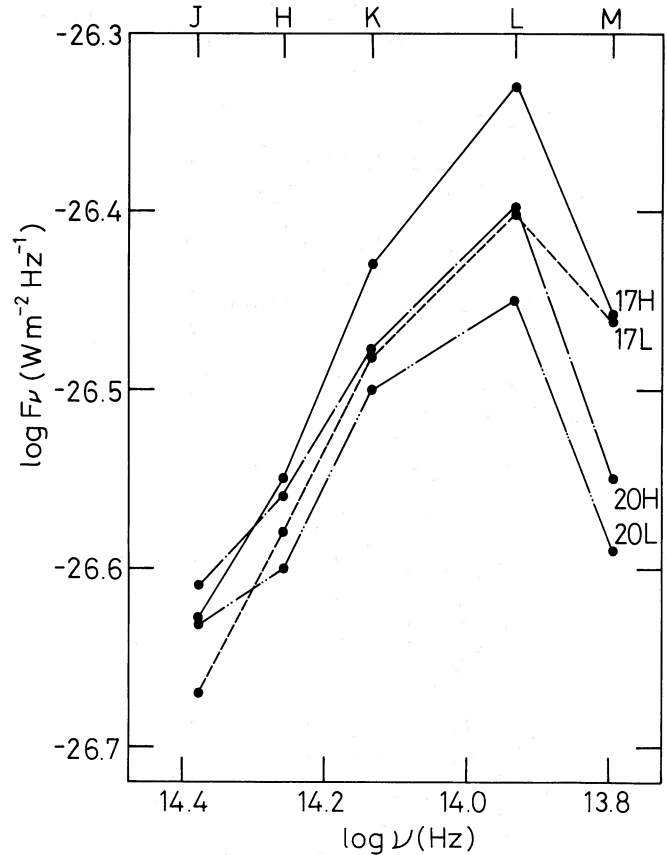
FIG. 5a

FIG. 5b

FIG. 5.—Day-to-day variation in the IR flux distribution of SS 433. (a) Weighted mean values for the nights July 17 through 22 (UT); (b) "high" state and "low" state, separately for July 17 and 20 (UT). Note that the weighted night mean depends on the frequency of observation during the specific state and the signal-to-noise ratio of individual data. The accuracy of the M band data is substantially lower than that of the data in the other bands, and the weight of the data for July 18 is very low; see Table 1.

fluxes; during our observing run in 1983 July, for which $\Psi_{164} = 0.923$–0.961, the excess appeared around $\phi_{13} \approx 0.1$, remained over the faint phase around $\phi_{13} \approx 0.2$, and disappeared around $\phi_{13} \approx 0.3$. The scatter of the data points in the middle panels of Figures 1 and 2 suggests that the details of day-to-day variations may vary from one period to another, although the global trend of the light curves remains similar. During our observations no "flare-ups" were recorded; Figures 3 and 4 indicate that less activity occurs for $-0.2 < \Psi_{164} < +0.2$.

V. DISCUSSION

The similarity of the optical and infrared light curves for the 164 day period strongly indicates that the main source of emission is the same in both regions and does not support the earlier view that the infrared radiation might be explained as free-free and bound-free emission from an extended region of H II gas surrounding the SS 433 system (Wynn-Williams and Becklin 1979; Giles et al. 1980). The present results may be interpreted with a binary model in which the observed fluxes are mostly attributed to an accretion disk around the compact star (Crampton, Cowley, and Hutchings 1980; Crampton and Hutchings 1981). The 164 day variation is interpreted in this model as due to the changing aspect of the accretion disk subjected to precession (Gladyshev 1981; Mazeh, Leibowitz, and Lahav 1981). The infrared data may contribute to refine the cylindrical disk model with a constant surface brightness

which was adopted by Leibowitz (1984) in order to interpret the UBV data of SS 433. The small amplitude of variation in the infrared compared to the optical region suggests a disk with varying effective temperature, because the infrared radiation is expected to originate predominantly in the extended cool outer part of disk, the visibility of which suffers less from changes in aspect than that of the hot inner part. This is especially true if the geometrical thickness of the disk increases outward. The "hump" around phase $\Psi_{164} \approx 0.2$–0.3 may be due to a hot spot that develops on the portion of the outer edge of the disk most easily seen around $\phi_{13} \approx 0.1$. The roughly similar height of the "hump" in the infrared and optical light curves (in both the 164 day and 13.08 day periods) indicates that the hot spot has a color close to that of the averaged disk at this phase.

In order to follow the location of the suspected "hot spot" on the disk, we drew isophote maps in a two-dimensional domain of (ϕ_{13}, Ψ_{164}) using 114 data points of the present observation, Giles et al. (1980), and Catchpole et al. (1981). We first made a two-dimensional Fourier analysis to determine the amplitudes of the cross terms of sin or cos $(2\pi n\phi_{13})$ and sin or cos $(2\pi m\Psi_{164})$ up to $n = 2$ and $m = 2$. The isophote maps were then constructed based on the light levels using these Fourier components. The map for the K band is shown in Figure 6. The ridge corresponding to the brightest phase runs from the lower left to the center, with an interruption around $\phi_{13} \approx 0.3$ due to the eclipse. The fact that the gradient $\Delta\phi_{13}/\Delta\Psi_{164}$ of the
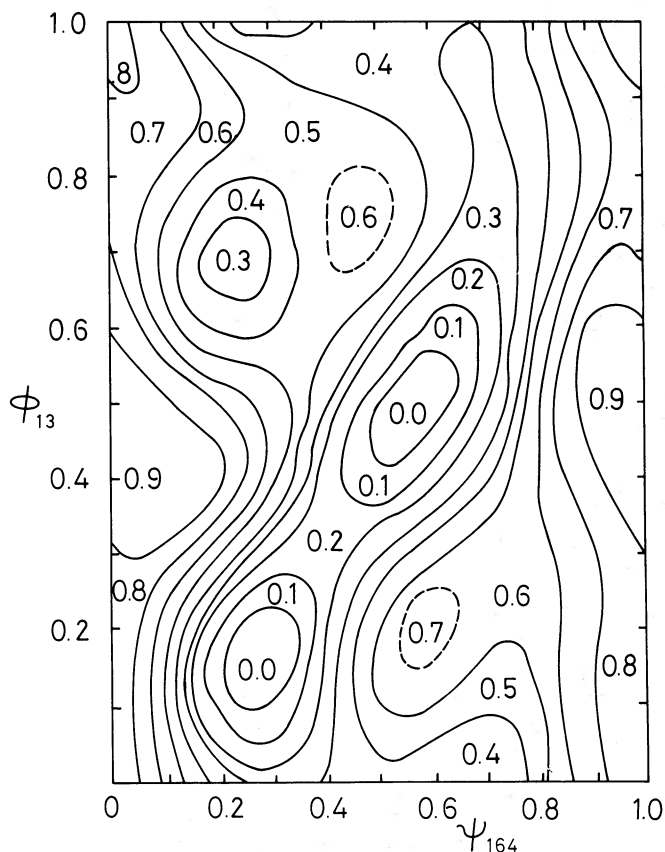
FIG. 6.—K isophote map in the two-dimensional phase domain. The isophote curves are based on the light levels reproduced by the two-dimensional Fourier analysis of the 114 raw data points of the present observations, Giles *et al.* (1980), and Catchpole *et al.* (1981). Note the ridge running from the lower left to the center. It may be regarded as a "hot-spot" effect in the case of the accretion disk model. The isophote levels show relative K magnitudes.

(i.e., the location revolves to the back side of the disk) or both. The above conclusion is similar to that obtained from the model analysis of the V band light curves by Leibowitz (1984) but suggests a *prograde* precession in contrast to the latter for a retrograde case. We have applied a two-dimensional Fourier analysis as above also to the V data in Leibowitz *et al.* (1984) but cannot detect clear ridgelike structure indicating a retrograde precession. Since the Fourier fitting might be affected by inhomogeneous distribution of data points over the two-dimensional space, more infrared observations are desirable.

The shallowness of the eclipse minima of the infrared light curves suggests that the majority of the infrared flux is emitted by the disk which eclipses the normal star at $\phi_{13} = 0.73$ and that the normal star eclipses only a small part of the extended infrared disk at $\phi_{13} = 0.23$.

The argument for the "B star" model is based on the energy distribution in the optical-infrared region, which can be approximated by blackbody radiation of about 24,000 K with reddening of $A_V \approx 9$ rather than by the standard disk model following the $v^{1/3}$ law, which should have higher infrared flux than observed (Murdin, Clark, and Martin 1980). Clark and Milone (1981) pointed out the slight excess of the observed flux relative to the blackbody model for $\lambda > 3$ μm, which was then attributed to hot gas surrounding the B star. The present data in Figure 5 do not affect their conclusions. We would like, however, to remark that the $v^{1/3}$ law must be applied with care in the infrared region because the outer cutoff of the disk decreases the near-infrared flux if this takes place at a temperature of $T > 10^3$ K. Accordingly, one cannot eliminate the disk model solely by arguing from the lack of infrared flux.

The cause of the day-to-day variation may be sought in varying configurations of disk structures depending on the mass supply and the internal magnetohydrodynamic balances. The darkening with a time scale of hours represented by the "low state" observed on two nights is difficult to explain at this stage unless one invokes a sort of starspot on the disk.

ridge is close to unity suggests that the brightening occurs when, seen from the compact star, the noncompact companion passes through a fixed elongation relative to the disk line of nodes with the orbital plane, if the precession is prograde. The disappearance of the ridge for $0.8 \leq \phi_{13} \leq 1.0$ may be interpreted as a physical decline of this effect or as an aspect effect

REFERENCES

Beckwith, S., Evans, N. J., Becklin, E. E., and Neugebauer, G. 1976, *Ap. J.*, **208**, 390.
Catchpole, R. M., Glass, I. S., Carter, B. S., and Roberts, G. 1981, *Nature*, **291**, 392.
Clark, T. A., and Milone, E. F. 1981, *Pub. A.S.P.*, **93**, 338.
Crampton, D., Cowley, A. P., and Hutchings, J. B. 1980, *Ap. J. (Letters)*, **235**, L131.
Crampton, D., and Hutchings, J. B. 1981, *Ap. J.*, **251**, 604.
Giles, A. B., King, A. R., Jameson, R. F., Sherrington, M. R., Hough, J. H., Bailey, J. A., and Cunningham, E. C. 1980, *Nature*, **286**, 689.

Gladyshev, S. A. 1981, *Soviet Astr. Letters*, **7**, 330.
Kodaira, K., and Lenzen, R. 1983, *Astr. Ap.*, **126**, 440.
Leibowitz, E. M. 1984, *M.N.R.A.S.*, **210**, 279.
Leibowitz, E. M., Mazeh, T., Mendelson, H., Kemp, J. C., Barbour, M. S., Takagishi, K., Jugaku, J., and Matsuoka, M. 1984, *M.N.R.A.S.*, **206**, 751.
Margon, B. 1982, *Science*, **215**, 247.
Mazeh, T., Leibowitz, E. M., and Lahav, O. 1981, *Ap. Letters*, **22**, 185.
Milone, E. F., and Clark, T. A. 1979, *IAU Circ.*, No. 3354.
Murdin, P., Clark, D. H., and Martin, P. G. 1980, *M.N.R.A.S.*, **193**, 135.
Wynn-Williams, C. G., and Becklin, E. E. 1979, *Nature*, **282**, 810.

DANA E. BACKMAN: Kitt Peak National Observatory, Tucson, AZ　85726-6732

KEIICHI KODAIRA: Tokyo Astronomical Observatory, Mitaka, Tokyo PC 181, Japan

YOSHIKAZU NAKADA: Department of Astronomy, Faculty of Science, University of Tokyo, Bunkyo, Tokyo PC 113, Japan